Collective excitations in liquid para-H_2: A neutron polarization-analysis study

M. García-Hernández and F. J. Mompeán
Instituto de Ciencias de Materiales de Madrid, CSIC, Cantoblanco, E-28049 Madrid, Spain

O. Schärpf and K. H. Andersen
Institut Laue-Langevin, B.P. 156, F-38042 Grenoble Cedex 9, France

B. Fåk
Département de Recherche Fondamentale sur la Matière Condensée, SPSMS/MDN, CEA Grenoble, 38054 Grenoble, France

(Received 28 July 1998)

Neutron time-of-flight spectroscopy combined with polarization analysis has enabled the experimental separation of the coherent and spin incoherent contributions to inelastic scattering from liquid para-hydrogen. The results from this experiment are analyzed in terms of self and distinct molecular contributions and extend the range of the observed distinct response beyond the wave numbers corresponding to the first peak in the static structure factor of the liquid. The collective response is adequately described in terms of two damped harmonic oscillators. While the observed wave number dependences resemble acoustic longitudinal and optical branches in long-range-ordered systems, the possibility of a multiexcitation origin for the higher-energy branch cannot be ruled out on the basis of the present experimental evidence. [S0163-1829(99)13101-1]

I. INTRODUCTION

Despite the facts that inelastic neutron scattering has long been established as a powerful set of techniques to probe condensed matter, and that the conceptual framework provided by van Hove correlation functions[1] constitutes a unique theoretical tool for the study of disordered systems, the knowledge gained by this standard approach to the collective dynamics of the lightest molecular liquid has been rather limited. From the experimental point of view, the difficulties stem from the coexistence at low temperatures of the two varieties of H_2 molecules: para-H_2 (even rotational quantum numbers J, antisymmetric molecular nuclear spin states $I=0$) and ortho-H_2 (odd J, symmetric molecular nuclear spin state, $I=1$). In the liquid phase, once the equilibrium state is reached the amount of ortho-H_2 will range from less than 10^{-3}% at $T=13$ K to 4% at $T=32$ K. In the absence of catalyzers and at liquid temperatures, this equilibrium is reached with a characteristic $1/e$ time of the order of 190 h and any observation extending over that period of time, such as neutron inelastic scattering experiments, would actually correspond to a system with changing composition. Moreover, given the difference in the molecular nuclear spin states and given the disparity in the neutron-scattering lengths for the singlet and triplet neutron-proton compound states, the scattering cross sections for neutrons with incident energies above 14 meV by mixtures containing even 1% ortho-H_2 have an overwhelming spin-incoherent component. Since the degree of anisotropy of the intermolecular potential depends strongly on the quantum number J to the point of altering significantly the depolarized light scattering below $E=10$ meV,[2] such observations are not acceptable to draw conclusions on the physics of the system and neutron inelastic-scattering measurements on this liquid close to the quantum limit and holding anisotropic interactions are still out of the present limits of the neutron technique. The use of catalyzers to accelerate the attainment of the equilibrium composition corresponding to the chosen temperature in the liquid range yields ortho-para mixtures where any significant intermolecular interactions are isotropic but which are still sufficiently rich in the first kind of molecules to give rise to a significant degree of incoherent scattering. As a direct consequence, in conventional neutron inelastic-scattering studies, i.e., without polarization analysis, the collective dynamics are observed not only through their contribution to the coherent dynamical structure factor $S_{coh}(Q,E)$, but also projected on the individual contributions of the molecules constituting the incoherent structure factor $S_{incoh}(Q,E)$. The result is complex spectra and a correspondingly high uncertainty in the conclusions drawn from the analysis.

In a liquid mixture enriched in para-H_2, using line-shape analysis and proposing a model for $S_{coh}(Q,E)$, we have recently reported the dispersive behavior of collective excitations of longitudinal acoustic character and the existence of a second contribution to the scattering at higher excitation energies whose nature could not be determined unambiguously.[3] These latter results are obtained by three-axis spectrometry with unpolarized neutron beams and follow earlier efforts to characterize the dispersive behavior and the range of existence of collective excitations in this liquid.[4] Even though the liquid hydrogens are relatively close to the quantum limit in their translational degrees of freedom, assuming that the individual molecules behave as distinguishable particles that obey Boltzmann statistics in the liquid phase allows the partition of the coherent and incoherent dynamical scattering functions into *self*, $S_s(Q,E)$, and *distinct*, $S_d(Q,E)$, molecule components. The uncertainty placed on our previous results by the lack of direct experimental access to $S_d(Q,E)$ can be alleviated by the use of neutron classical polarization analysis, as was early recognized.[5] The ability of this technique to discriminate between coherent and spin-incoherent scattering[6] can be ap-

plied advantageously to the study of the liquid hydrogen atoms as will be discussed below. The recourse to polarization analysis, however, is not free from a number of trade-offs apart from the obvious one of the loss of beam intensity. Presently, there is a very small number of neutron inelastic spectrometers combining time-of-flight (TOF) techniques and polarization analysis. The use of supermirror polarizers[7] in these devices also places a further restriction on the range of incident energies for which polarized beams are available and the result is a limited coverage of the (Q,E) space. For our particular application, however, the existing experimental window seems adequate both on the basis of the results of our previous study and from the theoretical standpoint. The quantum variational prediction for the wave number dependence of the elementary excitations (dispersion relation) of this liquid near the triple point available[8] within the correlated density matrix approach predicts the existence of a minimum in the dispersion relation near $Q=2$ Å^{-1}, which resembles the well-known ''roton'' minimum in liquid ^{4}He.

II. EXPERIMENTAL PART

A. Sample preparation

The H_2 sample enriched in para-H_2 was prepared from high-purity commercially available (Alphagaz N99) H_2 gas. The gas was condensed over IONEX O-P catalyst (available from The IONEX Research Corporation, Broomfield, Colorado) kept at a temperature of 15 K in the bottom of an aluminum sample container placed inside a cryostat. The ferric oxide catalyst accelerates the conversion process of the initially normal mixture of H_2 to a composition close to the equilibrium concentration at the experimental temperature (99.98% para-H_2). The measurements were performed at a temperature of 16 K under saturated vapor pressure from which a corresponding sample density of 0.037 mol/cm^3 was inferred from equation of state data.[11] An independent experimental check of the quoted ortho-H_2 concentration can be obtained by comparison of the energy-integrated spin-flip intensities at low scattering angles from the sample and the known amount of Al in the empty container. As in our previous study and in order to reduce neutron multiple scattering, the cylindrical cell (1.5 cm diameter, 5 cm height) was divided into five shorter cylinders of approximately 1 cm height by means of the insertion of Cd spacers lying parallel to the instrument scattering plane. The ortho-para conversion catalyst was masked by means of a Cd strip attached to the bottom of the cell. Particular attention was paid to the absence of magnetic materials in the sample environment which could alter the polarization state of the neutrons by continuously monitoring the flipping ratio of the throughgoing beam.[12] Background measurements correspond to measurements taken once the sample container was evacuated from its hydrogen content, but with the rest of the sample experimental setup in place.

B. Instrumental details and polarization analysis methodology

The experiments reported in this paper have been performed on the D7 spectrometer at the Institute Laue-Langevin (Grenoble, France) with an incident neutron energy $E_i=8.60$ meV (equivalent to a neutron wavelength of $\lambda=3.08$ Å). The instrument combines time-of-flight neutron energy analysis with a multidetector and supermirror polarization analysis and has been described in detail before.[13] The fundamentals of the method employed for the separation of coherent and spin incoherent neutron scattering in this type of instrument have been derived in Ref. 14 in the broader context of the separation of nuclear and magnetic contributions to the scattering. The complete set of measurements includes the determination in the same experimental setup of (ϕ denotes the scattering angle): (i) the spin-flip ratio of the polarization analysis setup using a purely coherent and diffuse scatterer (quartz glass rod) without time-of-flight energy analysis, $R(\phi)$; (ii) spin-flip, $I_{SF}(\phi,t)$, and non-spin-flip, $I_{NSF}(\phi,t)$, scattering intensities from the sample and background (with TOF energy analysis); (iii) the determination of the scattering intensity from the sample and background without analyzer stage, $I(\phi,t)$, (with TOF energy analysis); and (iv) calibration measurements (vanadium normalization runs). As described in Ref. 13, and after background subtraction and vanadium normalization, the corrected sample spin-flip, $I_{SF}^{corr}(\phi,t)$, and non-spin-flip, $I_{NSF}^{corr}(\phi,t)$, scattering intensities are calculated from

$$I_{SF}^{corr}(\phi,t)=I_{SF}(\phi,t)-\frac{1}{R(\phi)-1}[I_{NSF}(\phi,t)-I_{SF}(\phi,t)], \tag{1}$$

$$I_{NSF}^{corr}(\phi,t)=I_{NSF}(\phi,t)+\frac{1}{R(\phi)-1}[I_{NSF}(\phi,t)-I_{SF}(\phi,t)]. \tag{2}$$

These corrected scattering intensities comprise, however, a neutron wavelength transmission efficiency factor from the analyzer stage, $A(\phi,t)$, which cannot be determined by the quartz glass spin-flip ratio determinations and which has to be estimated if the actual spin-flip and non-spin-flip contributions from the sample are to be obtained:

$$I_{SF}^{corr}(\phi,t)=A(\phi,t)I_{SF}^{sample}(\phi,t), \tag{3}$$

$$I_{NSF}^{corr}(\phi,t)=A(\phi,t)I_{NSF}^{sample}(\phi,t). \tag{4}$$

To circumvent this problem, it is helpful to consider that the sample scattering intensity without polarization analysis, $I(\phi,t)$, actually contains the sum of the spin-flip and non-spin-flip scattered intensities without the effect of the wavelength-dependent transmission coefficient,

$$I(\phi,t)=I_{SF}^{sample}(\phi,t)+I_{NSF}^{sample}(\phi,t), \tag{5}$$

so that if the wavelength-dependent $A(\phi,t)$ factors are canceled by defining the experimental ratios

$$R_{SF}(\phi,t)=\frac{I_{SF}^{corr}(\phi,t)}{I_{SF}^{corr}(\phi,t)+I_{NSF}^{corr}(\phi,t)}, \tag{6}$$

$$R_{NSF}(\phi,t)=\frac{I_{NSF}^{corr}(\phi,t)}{I_{SF}^{corr}(\phi,t)+I_{NSF}^{corr}(\phi,t)}, \tag{7}$$

then the sought experimental magnitudes can be obtained from

$$I_{SF}^{sample}(\phi,t)=R_{SF}(\phi,t)I(\phi,t), \tag{8}$$

$$I_{NSF}^{sample}(\phi,t)=R_{NSF}(\phi,t)I(\phi,t). \tag{9}$$

The experimental magnitudes $I_{SF}^{sample}(\phi,t)$ and $I_{NSF}^{sample}(\phi,t)$ can be transformed to a (ϕ,E) grid and then corrected for multiple-scattering and sample absorption effects using a modified version of the DISCUS Monte Carlo simulation program.[15] A subsequent transformation to a (Q,E) grid is performed so that data analysis can proceed with magnitudes directly proportional to the dynamic scattering functions, which we shall denote by $S_{SF}(Q,E)$ and $S_{NSF}(Q,E)$. The relation of the latter with the dynamic scattering functions introduced in the preceding section will be discussed in Sec. III of this paper.

III. DATA ANALYSIS

A. Theoretical background

The primary quantities determined in our experiment are $S_{SF}(Q,E)$ and $S_{NSF}(Q,E)$ which correspond essentially to the double-differential scattering cross sections with and without spin flip, respectively, as a function of momentum and energy transfer. For a system composed of H_2 molecules and neglecting the very weak magnetic scattering effects between the neutron and the nuclear dipole moments, spin flips of neutrons with a wavelength 4 times larger than the interatomic distance ($d=0.74$ Å) can only arise through interactions with the molecular nuclear spin operator. The formulas derived by Sarma[5] and Young and Koppel[16] are specially useful in this context since they make explicit allowance for the various intramolecular degrees of freedom, which translate themselves into an effective dependence of the neutron-scattering cross sections with intramolecular quantum numbers and momentum transfer. These formulas are derived under the assumption that the molecular nuclear spin operators of different molecules are not correlated in the liquid phase (i.e., the molecules are not ''aligned''). With $E_i=8.60$ meV, the neutrons cannot promote the $J=0$ to $J=1$ rotational transition (para-ortho conversion) which requires $E_{01}=14.7$ meV so that, in practice under our experimental conditions and subject to the approximations mentioned above, we can expect only neutron-scattering events in which the rotational quantum numbers of the individual molecules are not changed. For the residual population of $J=1$ ortho-H_2 molecules these transitions give rise to both nuclear spin-flip and non-spin-flip events and there is both coherent and incoherent scattering, while for the majority of the $J=0$ para-H_2 molecules in the sample, the scattering events will result in only coherent scattering:

$$\begin{aligned} S_{NSF}(Q,E) &= c_{ortho}\tfrac{1}{3}\sigma_{incoh}[j_0^2(Qd/2)+2j_2^2(Qd/2)]S_{incoh}(Q,E) \\ &+ c_{ortho}\sigma_{coh}[j_0^2(Qd/2)+2j_2^2(Qd/2)]S_{coh}(Q,E) \\ &+ c_{para}\sigma_{coh}j_0^2(Qd/2)S_{coh}(Q,E), \end{aligned} \tag{10}$$

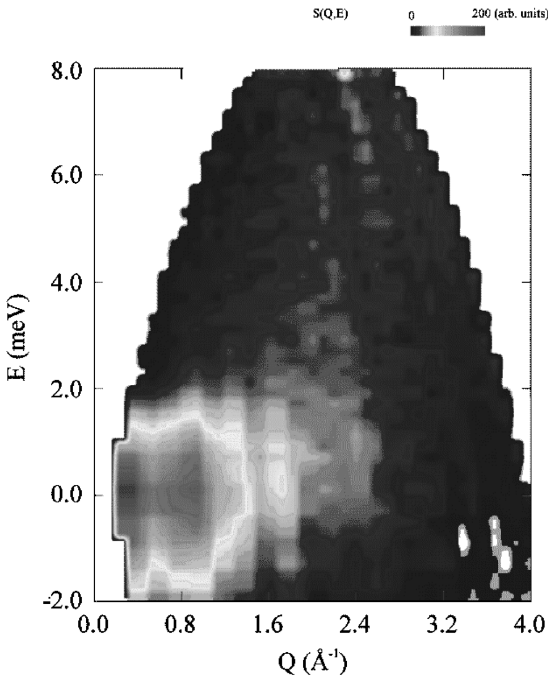

FIG. 1. Contour plot showing $\frac{3}{2}S_{SF}(Q,E)$ for liquid para-H_2 at $T=16$ K under saturated vapor pressure. See text for the precise relation of this magnitude to $S_{inc}(Q,E)$.

$$\begin{aligned} S_{SF}(Q,E) &= c_{ortho}\tfrac{2}{3}\sigma_{incoh}[j_0^2(Qd/2)+2j_2^2(Qd/2)] \\ &\times S_{incoh}(Q,E). \end{aligned} \tag{11}$$

In the above formulas, c_{ortho} and c_{para} denote the fractional concentrations of both types of molecules in the sample, $\sigma_{coh}=2.05$ b, $\sigma_{incoh}=78.7$ b, and the $j_l(x)$ are the spherical Bessel functions of order l. For the range of Q values covered in our experiment, the contributions arising from the second-order spherical Bessel function can be neglected. Figures 1 and 2 show, respectively, contour plots of the experimental magnitudes $\frac{3}{2}S_{SF}(Q,E)$ and $S_{NSF}(Q,E)-\frac{1}{2}S_{SF}(Q,E)$, which, neglecting the diatomic form factors and fractional concentrations, are close approximations to $S_{incoh}(Q,E)$ and $S_{coh}(Q,E)$ and show in a relatively model-free fashion the extent of the experimental separation achieved by neutron polarization analysis. For our quantitative analysis, we used Eqs. (10) and (11) to determine individually $S_{incoh}(Q,E)$ and $S_{coh}(Q,E)$. Once these magnitudes have been obtained, two further assumptions, namely, (i) that the molecules can be treated, at least in their translational degrees of freedom, as distinguishable Boltzmann particles and (ii) that the c_{ortho}/c_{para} ratio is known, allow the introduction of the self, $S_s(Q,E)$, and distinct, $S_d(Q,E)$, contributions to the dynamic scattering function:

$$S_{incoh}(Q,E)=S_s(Q,E), \tag{12}$$

$$S_{coh}(Q,E)=S_s(Q,E)+S_d(Q,E). \tag{13}$$

Through double space-time Fourier transformation, the latter scattering functions can be related to the corresponding van Hove correlation functions:

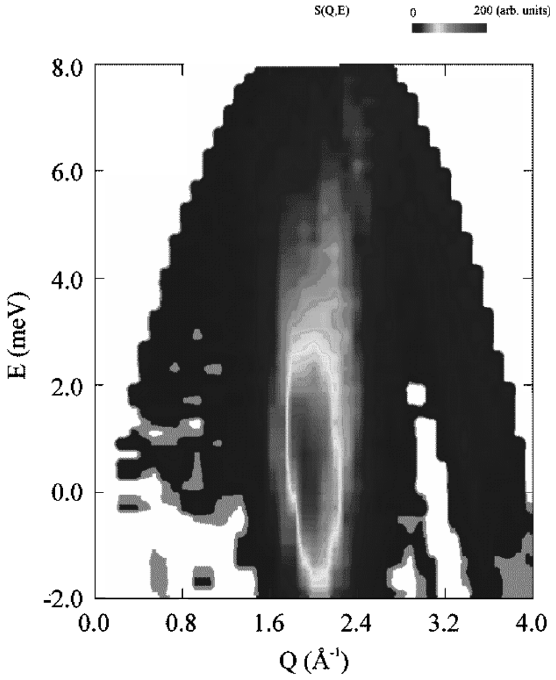

FIG. 2. Contour plot showing $S_{NSF}(Q,E)-\frac{1}{2}S_{SF}(Q,E)$ for liquid para-H_2 at $T=16$ K under saturated vapor pressure. See text for the precise relation of this magnitude to $S_{coh}(Q,E)$. Same color coding as in Fig. 1.

$$S_s(Q,E)=\frac{1}{2\pi}\int\int e^{[i(\mathbf{Q}\cdot\mathbf{R}-Et/\hbar)]}G_s(\mathbf{R},t)dtd^3\mathbf{R}, \quad (14)$$

$$S_d(Q,E)=\frac{1}{2\pi}\int\int e^{[i(\mathbf{Q}\cdot\mathbf{R}-Et/\hbar)]}G_d(\mathbf{R},t)dtd^3\mathbf{R}. \quad (15)$$

Note that as an additional assumption, we are not contemplating the possible dependence of the *self* and *distinct* van Hove correlation functions on the intramolecular quantum numbers.

B. Comment on $S_s(Q,E)$

The broad instrumental resolution function (triangular line shape with full width at half height of 3 meV) precludes any quantitative analysis of the $S_s(Q,E)$ surface. The observed scattering is found to consist of a single spectral component centered at $E=0$ throughout all the accessible range of momentum transfers and originating in the translational diffusion of single $J=0$ molecules.

C. Model for $S_d(Q,E)$

In order to interpret the experimentally determined $S_d(Q,E)$ it is useful to compare it, by means of nonlinear least-squares-fitting procedures, to models suited to the particular region of energy and momentum transfer which has been sampled. The models need to be convoluted with the instrumental resolution function. Figures 3 and 4 show plots of $S_d(Q,E)$ at constant values of Q. The strong line-shape asymmetry shown by the $Q=1.8$ and 2.0 Å^{-1} spectra, suggestive of two broad spectral components of different relative intensities, leads to two clear maxima for $Q=2.2$ and 2.4 Å^{-1}. This observation is consistent with the results of

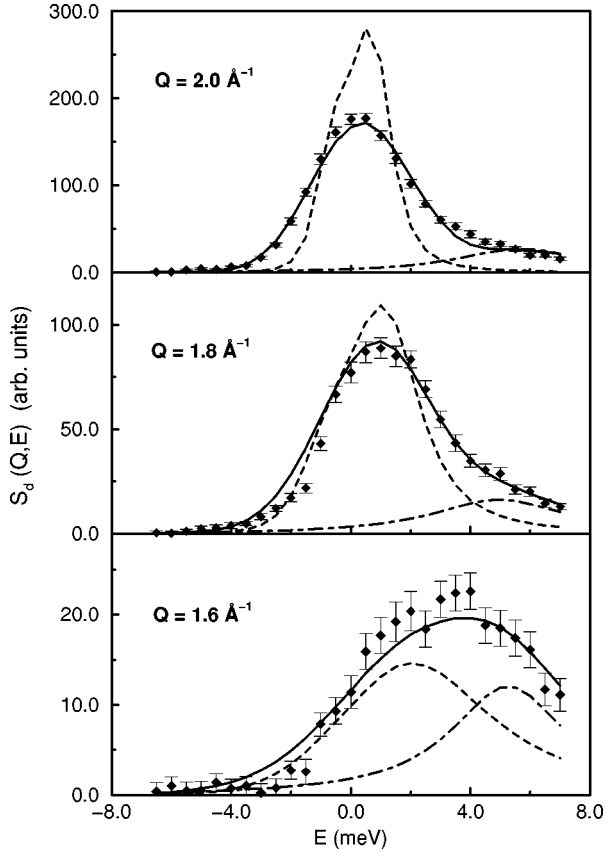

FIG. 3. Constant-Q cuts of $S_d(Q,E)$ for liquid para-H_2 at $T=16$ K under saturated vapor pressure. Solid diamonds are fully corrected experimental data. The solid line represents the best fit to these data, consisting of the convolution with the instrumental resolution of the two damped harmonic oscillator model discussed in the text. Individual damped harmonic oscillator contributions are indicated by the dashed line ($i=1$) and dot-dashed line ($i=2$).

our previous study,[3] where we found that for the range $0.6 \leqslant Q \leqslant 2.0$ Å^{-1} the experimental data on $S(Q,E)$ were compatible with $S_d(Q,E)$ being represented by a sum of two damped harmonic oscillator (DHO) terms,[17] each corresponding to the individual collective modes presumed to contribute to the spectra:

$$S_d(Q,E)=[n(E)+1]\sum_{i=1}^{N=2} Z_i(Q) \times \frac{4EE_{i,Q}\Gamma_{i,Q}}{(E^2-\Omega_{i,Q}^2)^2+4E^2\Gamma_{i,Q}^2}. \quad (16)$$

Here $E_{i,Q}$ stands for the bare energy of oscillator i, $\Gamma_{i,Q}$ stands for the damping parameter in energy units, the renormalized energy is given by $\Omega_{i,Q}=(E_{i,Q}^2+\Gamma_{i,Q}^2)^{1/2}$, $Z_i(Q)$ represents the oscillator strength, and $[n(E)+1]$ is the Bose occupation factor. In Ref. 3 a model with only one DHO ($N=1$) was found to be valid below $Q=1.6$ Å^{-1}, but above this value of momentum transfer, a second DHO improved significantly the goodness of the fit.

As shown in Figs. 3 and 4, the spectral features obtained from our polarization analysis can also be adequately described by including two DHO in the model for $S_d(Q,E)$.

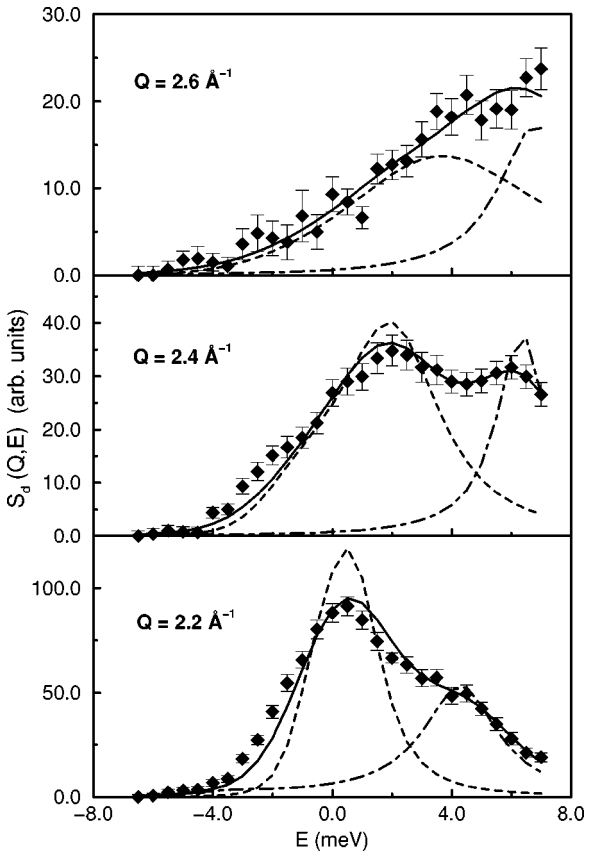

FIG. 4. Constant-Q cuts of $S_d(Q,E)$ for liquid para-H_2 at $T=16$ K under saturated vapor pressure. Symbols as in Fig. 3.

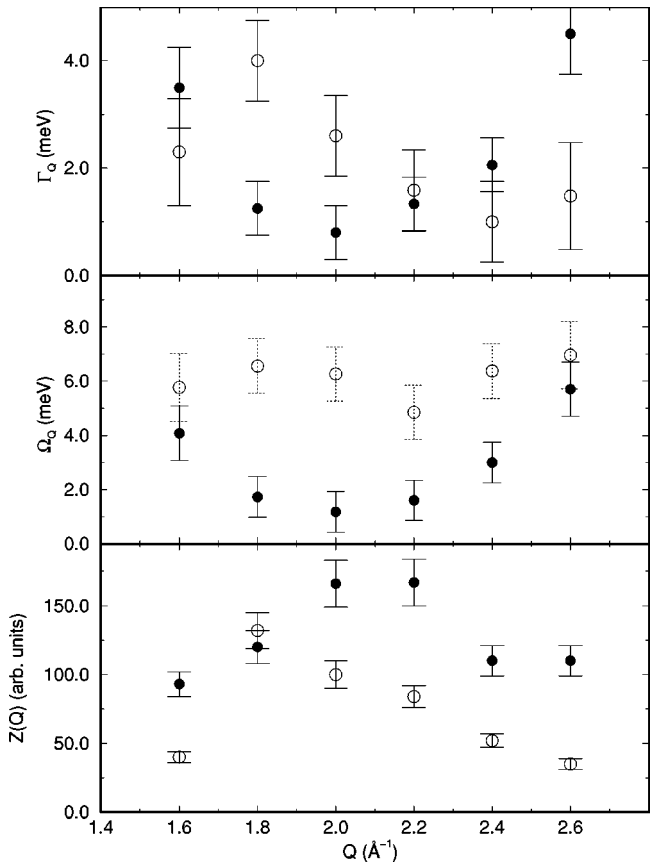

FIG. 5. Q-dependence of the best fit model parameters. Solid circles refer to the first damped harmonic oscillator and open circles to the second one. The $Z_i(Q)$ intensity parameters are shown in (a). Renormalized energies are shown in (b) and damping coefficients are shown in (c).

The best fitting parameters show the Q dependences illustrated in Fig. 5. The values of the renormalized frequencies for the first DHO ($i=1$) show a minimum near $Q=2$ Å^{-1}, where the corresponding oscillator strength reaches its maximum value. This leads to the identification of the excitation as the analog in the liquid of a longitudinal acoustic mode in a periodic medium. An immediate result from data obtained with polarization analysis is that the need to include a second DHO in our partition of $S_d(Q,E)$ rules out our previous speculation of the extra contribution being due to a single-particle density-of-states term. Both DHO's are found to be not overdamped [the overdamped regime being defined as $\Gamma_Q^2/\Omega_Q^2>1$ (Ref. 17)].

IV. DISCUSSION

As mentioned in the Introduction, our access to the (Q,E) space in the experiment reported in this paper has been limited to a region near $Q=Q_P=2$ Å^{-1} where a first maximum in the liquid static structure factor, arising from first-neighbor molecular contributions, is expected. For this reason, we digress first on the direct consequences of our reported experimental data and then examine them in the context of those extracted from neutron spectroscopy without polarization analysis. Finally, we relate our results to those obtained on other hydrogen liquid mixtures.

Our experimental approach has enabled the experimental separation of the coherent and incoherent dynamical scattering functions. To the limit of our knowledge this is the first time that this separation has been reported for a molecular fluid composed of small molecules. We remark here that despite the closeness to the quantum regime in the translational degrees of freedom, our analysis has shown that the classical partition into distinct and self scattering contributions seems to be valid within the limits of our experimental uncertainties. The observed qualitative behavior for the renormalized frequency of the first DHO agrees well with the observations made in other liquids, both in the classical and quantum regimes, reflecting the lower cost in energy needed to create relatively short-lived collective excitations when their wavelengths approach the accredited distance between first-neighboring molecules.[18]

From a theory-of-liquids perspective, the confirmation of the collective character of the response being modeled through the second DHO would imply the breakdown of the single-mode approximation for the analysis of the neutron response in this system, provided that it cannot be assigned to a multiexcitation contribution. This point cannot be resolved on the basis of the present experimental evidence, which does not explore the dependence on the thermodynamic conditions of the neutron response. However, estimates of the double-excitation contributions, corresponding to the first DHO, can be made following Graf *et al.*[19] It is found that the latter is more prominent for energy transfer values corresponding to multiples and combinations of the

local maxima and minima in the single-excitation dispersion relation. Given the fact that renormalized energies for the second DHO, $\Omega_{2,Q}$, do not seem to correspond to any of this favored combinations and since the observed spectral features are of noticeable intensity, we explore an alternative explanation. Since the values for $\Omega_{2,Q}$ resemble those expected for a branch of optical character near the origin of the second Brillouin zone in a single crystal, we draw further the known analogy between the liquid response and that corresponding to a polycrystalline average. We recall that for polycrystals, first-principles calculations for monoatomic Lennard-Jones systems by de Wette and Rahman[20] early found that an average dispersion curve was not a good description for wave vectors in excess of the values corresponding to Bragg peaks. This average dispersion relation showed a nonzero minimum near the position of the corresponding to the first Bragg peak, resembling our experimental findings near $Q=2$ Å^{-1}. Similar behavior is expected in isotropic amorphous materials where model calculations for acoustic modes[21,22] show a finite-energy distinct response with a minimum near Q_P due to diffuse Umklapp scattering, mainly from transverse acoustic excitations.

In agreement with previous observations in liquid normal D_2,[9,10,23] the wave vector dependence near Q_P seems to be well accounted for by a parabolic dependence of the type proposed by Landau in the context of roton excitations in ^{4}He, with an excitation gap, $\Delta_{H_2}=1.65$ meV$\cong\Delta_{D_2}/\sqrt{2}$, where $\Delta_{D_2}=2.26$ meV is the value recently reported[23] for liquid normal D_2 near its triple point. The comparison of the results for the two liquids can be understood if we assume the existence of a diffuse Brillouin zone limit near $Q_P/2$, within the time scales probed by neutrons in our experiment, where the dispersive behavior shown in the low-Q limit is reflected. Normal liquid D_2 showing, near its triple point, a positive dispersion leads to higher excitations energies near Q_P than those found in liquid para-H_2. To establish this conclusion, we need to gauge our degree of confidence in the results obtained previously without polarization analysis. To this extent, Fig. 6 shows a composite picture of the results obtained from neutron-scattering experiments with and without[3] polarization analysis and the theoretical single-mode prediction near the triple point based in the correlated density matrix approach, taken from Ref. 8. We find that the overlap between the two sets of experimental data is very satisfactory, both for the first and second DHO's, and considerably reinforces our knowledge of the collective behavior near Q_P. Strictly speaking, the absence of polarization analysis results for $Q\leqslant 1.6$ Å^{-1} places higher uncertainties in the conclusion drawn about the fact that the hydrodynamic sound limit at low Q seems to be approached by the first DHO from low energies (negative dispersion), but it seems implausible that in this region of Q the observed branch should deviate from the previously reported behavior, which itself marks a striking difference with the observation of positive dispersion in liquid normal D_2.[9,10]

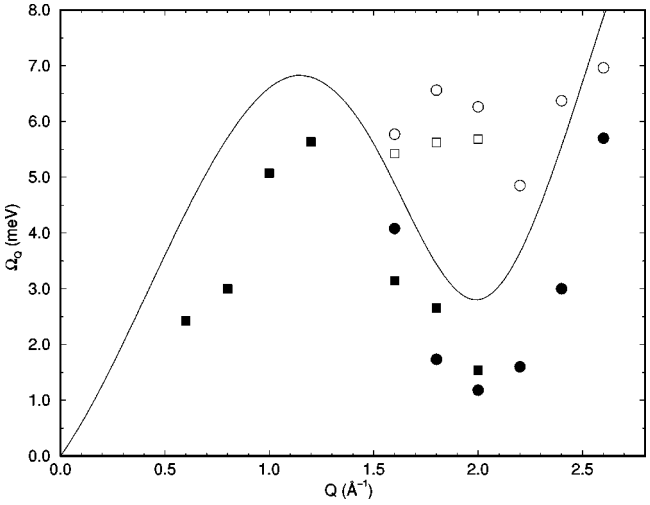

FIG. 6. An overall comparison of the existing experimental and theoretical data for the renormalized energies of the collective excitations in liquid para-H_2, plotted as a function of wave number. Squares are taken from three-axis neutron spectroscopy without polarization analysis (Ref. 3), solid squares refer to a first DHO and open squares to a second DHO. Circles refer to the present paper data: solid circles refer to a first DHO (longitudinal acoustical character) and open ones to a second DHO. The solid line represents the correlated density matrix result in the single mode approximation near the triple point, taken from Ref. 8.

V. CONCLUSIONS

The combination of time-of-flight neutron spectrometry with polarization analysis on a multidetector instrument has enabled the experimental separation of the coherent and incoherent contributions to the scattering double-differential cross sections from liquid para-hydrogen. From these, it has been possible to derive the distinct contribution to the dynamical scattering functions $S_d(Q,E)$ and study its wave number dependence near the first maximum of the structure factor of the liquid. Two branches have been identified, which agree well with those previously derived from line-shape analysis of experiments with unpolarized neutrons. One of the branches seems to represent collective excitations of longitudinal acoustic character. We propose that the second branch corresponds to collective excitations of optical character, although a multiexcitation origin cannot be ruled out. The existence, within the time scale explored in our experiment, of a diffuse Brillouin zone with limit around $Q_P/2$ seems to help to rationalize the observed distinct response and the comparison of the excitation gap values near Q_P for liquid para-H_2 and liquid normal D_2 near their respective triple points.

ACKNOWLEDGMENTS

The authors would like to thank Boris Toperverg for many fruitful discussions. This work was supported in part by Spanish DGICYT through Project No. PB92-0015.

[1] L. van Hove, Phys. Rev. **95**, 249 (1954).
[2] P. A. Fleury and J. P. McTague, Phys. Rev. Lett. **31**, 914 (1973).
[3] F. J. Mompeán, M. García-Hernández, and B. Fåk, Phys. Rev. B **56**, 11 604 (1997).
[4] W. Schott, Z. Phys. **231**, 243 (1970); K. Carneiro, M. Nielsen, and J. P. McTague, Phys. Rev. Lett. **30**, 481 (1973); K. Carneiro (unpublished); Phys. Rev. A **14**, 517 (1976).
[5] G. Sarma, *Inelastic Scattering of Neutrons in Solids and Liquids* (I.A.E.A., Vienna, 1961), p. 397.
[6] O. Schärpf, Physica B **182**, 376 (1992).
[7] O. Schärpf, Physica B **156–157**, 639 (1989).
[8] M. L. Ristig, G. Senger, and K. E. Kürten, in *Recent Progress in Many-Body Theories*, edited by A. J. Kallio *et al.* (Plenum, New York, 1988), Vol. 1, p. 197.
[9] F. J. Bermejo, F. J. Mompean, M. Garcia-Hernandez, J. L. Martinez, D. Martin-Marero, A. Chahid, G. Senger, and M. L. Ristig, Phys. Rev. B **47**, 15 097 (1993).
[10] F. J. Mompean, F. J. Bermejo, M. Garcia-Hernandez, B. Fåk, J. L. Martinez, G. Senger, and M. L. Ristig, J. Phys.: Condens. Matter **5**, 5743 (1993).
[11] H. M. Roder, G. E. Childs, R. D. McCarty, and P. E. Angerhofer (unpublished).
[12] O. Schärpf and I. Anderson, J. Neutron Res. **4**, 227 (1996).
[13] O. Schärpf, *Neutron Scattering in the 'Nineties* (I.A.E.A., Jülich, 1985), p. 85.
[14] O. Schärpf and H. Capellmann, Phys. Status Solidi A **135**, 359 (1993).
[15] M. W. Johnson (unpublished); O. Schärpf and B. Gabrys, in *Proceedings of the Seventh International School of Condensed Matter*, Bialystok, Poland, 1997, edited by K. Perzynska and L. Dobrzynski (Institute of Physics, Bialystok, 1997), p. 119.
[16] J. A. Young and J. U. Koppel, Phys. Rev. **135**, A603 (1964).
[17] B. Fåk and B. Dorner, Physica B **234–236**, 1107 (1997).
[18] J. P. Boon and S. Yip, *Molecular Hydrodynamics* (McGraw-Hill, New York, 1980), pp. 279ff.
[19] E. H. Graf, V. J. Minkiewicz, H. Bjerrum-Moeller, and L. Passell, Phys. Rev. A **10**, 1748 (1974).
[20] F. W. de Wette and A. Rahman, Phys. Rev. **176**, 784 (1968).
[21] J. M. Carpenter and C. A. Pelizzari, Phys. Rev. B **12**, 2391 (1975).
[22] J. Hafner, J. Phys. C **14**, L287 (1981).
[23] M. Mukherjee, F. J. Bermejo, B. Fåk, and S. M. Bennington, Europhys. Lett. **40**, 153 (1997).